

基于香豆素的增强型铜离子荧光探针及其在细胞成像中的应用

张长丽* 张 虹 何凤云 杨 慧 刘少贤 柳闽生

(南京晓庄学院环境科学学院, 南京市先进功能材料重点实验室, 南京 211171)

摘要: 以香豆素为荧光团, 设计合成了一种反应型铜离子荧光探针 **Cou-P**。**Cou-P** 对 Cu^{2+} 表现出高选择性、荧光增强性识别。分别用紫外可见光谱、荧光光谱、质谱等方法研究了 **Cou-P** 识别 Cu^{2+} 机理, 结果表明 **Cou-P** 先形成 **Cou-P**/ Cu^{2+} (1:1) 配合物, **Cou-P**/ Cu^{2+} 配合物进一步被过量的 Cu^{2+} 催化水解为 3-(carboxylic acid)-7-(diethylamino)-coumarin (**Cou-COOH**)。另外, **Cou-P** 表现出低细胞毒性、良好的过膜性能, 成功地用于 MCF-7 细胞中 Cu^{2+} 检测。

关键词: 香豆素; 铜探针; 机理; 细胞造影

中图分类号: O614.121

文献标识码: A

文章编号: 1001-4861(2019)10-1869-08

DOI: 10.11862/CJIC.2019.207

Coumarin-Based Turn-on Fluorescent Probe for Copper(II) Detection and Its Application in Cell Imaging

ZHANG Chang-Li* ZHANG Hong HE Feng-Yun YANG Hui LIU Shao-Xian LIU Min-Sheng

(Key Laboratory of Advanced Functional Materials of Nanjing, School of Environmental
Science, Nanjing Xiaozhuang University, Nanjing 211171, China)

Abstract: A new coumarin-based Cu^{2+} probe (**Cou-P**) according to the Cu^{2+} -coordination induced hydrolysis mechanism has been developed. **Cou-P** exhibits a highly selective turn-on response to Cu^{2+} over other transition metal ions in aqueous media. The recognition mechanism of **Cou-P** for Cu^{2+} was confirmed by UV-Vis, fluorescence and mass spectrometry. The results show that **Cou-P** first forms **Cou-P**/ Cu^{2+} (1:1) complex, and **Cou-P**/ Cu^{2+} complex is further catalyzed to 3-(carboxylic acid)-7-(diethylamino)-coumarin (**Cou-COOH**) by excessive Cu^{2+} . **Cou-P** has low cytotoxicity and good membrane permeability. It has been successfully used to detect Cu^{2+} in MCF-7 cells.

Keywords: coumarin; copper probe; mechanism; cell imaging

0 Introduction

Fluorescent sensing of chemical species of biological and environmental significance by fluorescence spectroscopy has emerged as an attractive field for scientists, especially inspired by the development of confocal microscope and optical imaging techniques^[1-7]. As the third most abundant transition metal

ions in the human body, copper ions play important roles in various biological processes, and maintaining its homeostasis is critical for development of living organisms^[8-12]. The disturbed homeostasis of copper ions can result in severe cell damage and further lead to many diseases such as Menkes syndrome, Wilson disease, and Alzheimer disease^[13-21]. Due to its essential toxic nature, long-term exposure to high levels of

收稿日期: 2019-06-01。收修改稿日期: 2019-07-19。

江苏高校青蓝工程项目和南京晓庄学院校级科研项目(No.2018NXY49)资助。

*通信联系人。E-mail: carbon314@163.com

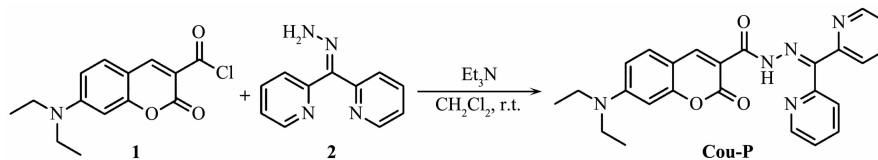
copper has been reported to induce the liver and kidney damage^[22]. According to the World Health Organization (WHO) International Standard for drinking water, the maximum acceptable level of copper in drinking water is $30 \mu\text{mol} \cdot \text{L}^{-1}$ ^[23]. Considering the important roles of copper in physiological processes and its high toxicity, development of specific fluorescent probes for sensitive copper detection, especially in environmental and physiological conditions is of great significance.

To date lots of fluorescent probes have been reported for Cu^{2+} detection based on two main mechanisms: coordination of receptor with Cu^{2+} ^[24-34] and Cu^{2+} -triggered specific reactions^[35-47]. Due to the paramagnetic nature of Cu^{2+} , Cu^{2+} coordination often results in fluorescence quenching. Fluorescence “turn-off” signals are usually less sensitive and generate false-positive results^[24,48], which is a disadvantage for practical application. Such obstacles can be eliminated by employing reaction-based probes, which achieve fluorescence “turn-on” response and offer

high selectivity by reacting specifically with Cu^{2+} to generate fluorescent products. However, few fluorescence turn-on Cu^{2+} probes have been reported^[49-54], which make the development of new fluorescence turn-on Cu^{2+} probes highly desired.

In this paper, **Cou-P**, a turn-on fluorescent probe for Cu^{2+} sensing based on a mechanism of Cu^{2+} -coordination-induced hydrolysis of hydrazides was developed. **Cou-P** exhibits a selective and sensitive emission turn-on response to Cu^{2+} and features visible light excitation and emission profiles. Moreover, its turn-on imaging ability for intracellular Cu^{2+} has been confirmed in human breast adenocarcinoma cells (MCF-7 cells) using a confocal microscope.

The synthesis route for **Cou-P** was depicted in Scheme 1. **Cou-P** was synthesized by reacting of 7-(diethylamino)-coumarin-3-carbonyl chloride and 2,2'-(hydrazonomethylene)dipyridine in the presence of Et_3N in a high yield (85%). It was well characterized by ^1H , ^{13}C NMR and ESI-MS (Supporting Information).



Scheme 1 Synthesis of **Cou-P**

1 Experimental

1.1 General procedures

All chemicals and solvents were of analytical grade or spectroscopic grade and were used without further purification. Dichloromethane was refluxed with calcium hydride and distilled at ambient pressure. ^1H NMR and ^{13}C NMR spectra were recorded on a Bruker DRX-300 spectrometer or Bruker DRX-500 spectrometer with TMS as internal reference in CDCl_3 . Mass spectrometric data were determined with LCQ ESI-MS Thermo Finnigan mass spectrometer. Absorption spectra were measured on a Shimadzu UV-3100 UV-Vis-NIR spectrophotometer. The fluorescence spectra were recorded with an AMINCO Bowman series 2 luminescence spectrophotometer (cuvette, 1

cm) with a xenon lamp as the light source.

1.2 Synthesis of Cou-P

A solution of compound **1** (200 mg, 0.72 mmol) in CH_2Cl_2 (5 mL) was slowly added to a solution of compound **2** (143 mg, 0.72 mmol) and Et_3N (80 mg, 0.68 mmol) in CH_2Cl_2 (10 mL). The reaction mixture was stirred at room temperature for 24 h. The mixture was washed with water (3×15 mL). The organic layer was dried on MgSO_4 and filtered, and the filtrate was concentrated to dryness. The crude product was purified by column chromatography (silica gel, $V_{\text{MeOH}}: V_{\text{CH}_2\text{Cl}_2}=1:10$, $R_f=0.4$), and pure compound **Cou-P** was obtained as an orange solid (270 mg) in 85% yield. ^1H NMR (400 MHz, CDCl_3): δ 8.97 (d, 1H, $J=4.0$), 8.83 (s, 1H), 8.58 (d, 1H, $J=4.0$), 8.28 (d, 1H, $J=8.0$), 7.86~7.78 (m, 2H), 7.52 (d, 2H, $J=8.0$), 7.46~7.30 (m, 2H),

7.28~7.31 (t, 1H, $J=4.0$), 6.63~6.66 (dd, 1H, $J_1=2.4$, $J_2=2.0$), 6.47 (s, 1H), 3.42~3.48 (q, 4H, $J_1=7.6$, $J_2=6.8$), 1.21~1.253 (t, 6H, $J=7.2$); ^{13}C NMR (100 MHz, CDCl_3): δ 161.92, 161.04, 158.12, 156.23, 153.04, 151.85, 149.45, 149.25, 149.07, 148.59, 136.86, 136.82, 131.53, 126.13, 124.18, 124.14, 123.70, 110.23, 110.16, 108.82, 96.84, 45.30, 12.59. ESI-MS (positive mode): Calcd. 905.90, Found: 905.08 for $[\text{2M}+\text{Na}]^+$. Element analysis Calcd. for $\text{C}_{25}\text{H}_{23}\text{N}_5\text{O}_3$ (%): C, 68.01; H, 5.25; N, 15.86. Found(%): C, 68.12; H, 5.46; N, 15.78.

1.3 Spectroscopic measurements

All the solvents were of analytic grade. The stock solution of **Cou-P** was prepared in CH_3OH ($1.04 \text{ mmol} \cdot \text{L}^{-1}$). For spectroscopic determination, the stock solution was diluted with PBS to the desired concentration. The stock solutions of metal ions were prepared by dissolving $\text{Cu}(\text{NO}_3)_2$, $\text{CoCl}_2 \cdot 6\text{H}_2\text{O}$, $\text{NiCl}_2 \cdot 6\text{H}_2\text{O}$, HgCl_2 , MnCl_2 , $\text{Fe}(\text{NO}_3)_3 \cdot 9\text{H}_2\text{O}$, $\text{FeSO}_4 \cdot 7\text{H}_2\text{O}$, AgNO_3 , PbCl_2 , $\text{Zn}(\text{NO}_3)_2 \cdot 7\text{H}_2\text{O}$, $\text{CdCl}_2 \cdot 2.5\text{H}_2\text{O}$, KCl , CaCl_2 , NaCl , $\text{MgCl}_2 \cdot 6\text{H}_2\text{O}$ with doubly distilled water. Fluorescence measurements of **Cou-P** ($10 \mu\text{mol} \cdot \text{L}^{-1}$) were performed with 4 nm slit for excitation and 4 nm slit for emission. The UV-Vis titration of **Cou-P** was carried out by adding aliquots of $2.5 \mu\text{L}$ of $\text{Cu}(\text{NO}_3)_2$ aqueous solution ($1.2 \text{ mmol} \cdot \text{L}^{-1}$) to 3 mL of probe solution ($10 \mu\text{mol} \cdot \text{L}^{-1}$) in a cuvette. The spectra were recorded after the solution was completely mixed. The fluorescence titration of **Cou-P** was also carried out by adding aliquots of $2.5 \mu\text{L}$ of $\text{Cu}(\text{NO}_3)_2$ aqueous solution ($1.2 \text{ mmol} \cdot \text{L}^{-1}$) to 3 mL of sample solution ($10 \mu\text{mol} \cdot \text{L}^{-1}$) in a cuvette. The measurements were carried out in 2 min after the addition. All experiments were carried out at 298 K.

1.4 Cell imaging

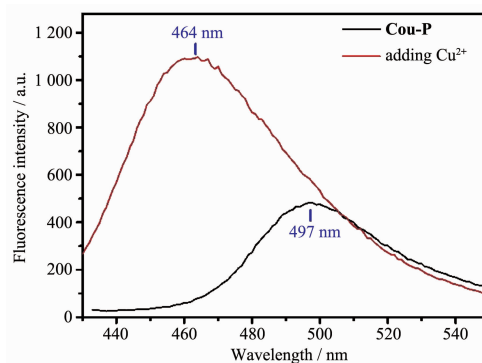
MCF-7 cells were cultured in Dulbecco's Modified Eagle Medium supplemented with 10% fetal bovine serum, penicillin ($100 \text{ unit} \cdot \text{mL}^{-1}$), streptomycin ($100 \text{ mg} \cdot \text{mL}^{-1}$) and 5% (V/V) CO_2 at 37°C . After removing the incubation media and rinsing with $1 \times \text{PBS}$ ($0.01 \text{ mol} \cdot \text{L}^{-1}$) for three times. The MCF-7 cells were incubated with **Cou-P** ($20 \mu\text{mol} \cdot \text{L}^{-1}$) for 30 min at 25°C . Then the cells were washed three times with $1 \times \text{PBS}$ and imaged with Zeiss LSM-710 microscope

equipped with a $63\times$ oil-immersion objective. For the imaging of MCF-7 cells upon incubation with exogenous Cu^{2+} , the exogenous Cu^{2+} was introduced by incubating the cells with $\text{Cu}(\text{NO}_3)_2$ ($200 \mu\text{mol} \cdot \text{L}^{-1}$) solution for 5 h at 25°C . The excitation wavelength of **Cou-P** used in experiment was 405 nm, while the filter was 420~520 nm.

2 Results and discussion

2.1 Sensing properties

The sensing ability of probe **Cou-P** for Cu^{2+} was investigated using fluorescence spectroscopy in HEPES buffer solution ($50 \text{ mmol} \cdot \text{L}^{-1}$, $0.1 \text{ mol} \cdot \text{L}^{-1}$ KNO_3 , $\text{pH}=7.2$). As shown in Fig.1, the probe **Cou-P** itself showed relatively weak fluorescence at 497 nm ($\Phi=0.005$) when excited by 460 nm. However, upon addition of 5 eq. of Cu^{2+} , probe **Cou-P** exhibited a significant fluorescence enhancement at 464 nm ($\Phi=0.068$), indicating that **Cou-P** could be efficiently responded in the presence of Cu^{2+} .



Excitation wavelengths are 460 nm for **Cou-P** and 400 nm for adding 5 eq. Cu^{2+} , respectively

Fig.1 Fluorescence spectra of **Cou-P** ($10 \mu\text{mol} \cdot \text{L}^{-1}$) and the corresponding hydrolysis product after adding 5 eq. Cu^{2+} in HEPES buffer ($50 \text{ mmol} \cdot \text{L}^{-1}$, $0.1 \text{ mol} \cdot \text{L}^{-1}$ KNO_3 , $\text{pH} 7.2$)

2.2 Mechanism study

Due to few reports on the reaction copper probes of hydrazide derivatives, the recognition mechanism of probe **Cou-P** for Cu^{2+} was investigated in detail. First, Cu^{2+} binding behaviour in **Cou-P** was investigated by fluorescent and UV-Vis titration experiments. The UV-Vis titration experiment demonstrates that free **Cou-P** has two main absorption bands centering at

454 ($\varepsilon=2.8\times10^4\text{ L}\cdot\text{mol}^{-1}\cdot\text{cm}^{-1}$) and 318 nm, which can be assigned to ICT and $\pi\text{-}\pi^*$ transition bands, respectively (Fig.2a). When Cu^{2+} was added, distinct reduction of the former band can be observed accompanied by the evident bathochromic shift to 474 nm, suggesting the increased coplanarity of electron-donating group induced by Cu^{2+} binding. Similar change was also observed for the latter band, yet the band shift is much less pronounced. The clear isosbestic points at 471, 396 and 339 nm imply the undoubted conversion of free **Cou-P** to a copper complex. The titration profile based on the former band shows that the absorbance descends linearly with $c_{\text{Cu}^{2+}}$ at the ratio of $c_{\text{Cu}^{2+}}/c_{\text{Cou-P}}\leq 1$. Higher $c_{\text{Cu}^{2+}}$ does not lead to any further evident change of isosbestic points at 471, 396 and 339 nm, suggesting a 1:1 stoichiometry for the copper complex. The result obtained from fluorescence Job's plot also confirms the 1:1 Cu^{2+} binding stoichiometry (Supporting information, Fig.S1). **Cou-P**/ Cu^{2+} complexes can remain stable for at least 120 min at pH 7.2 (Fig.S2). However, after the ratio of $c_{\text{Cu}^{2+}}/c_{\text{Cou-P}}$ attained 1, upon addition of another 0.1 eq. Cu^{2+} to the solution of **Cou-P**/ Cu^{2+} complex, a new absorption band centered at 414 nm appeared and the intensity enhanced gradually in a time-dependent manner; at the same time, the absorption band at 474 nm exhibited decrease (Fig.2b). The clear isosbestic points at 454 nm imply the undoubted conversion of **Cou-**

P/ Cu^{2+} complex to another compound. Normalized emission spectra of 3-(carboxylic acid)-7-(diethylamino)-coumarin (**Cou-COOH**) and **Cou-P** incubated with 1.1 eq. $\text{Cu}(\text{NO}_3)_2$ for 80 min overlapped well, **Cou-P**/ Cu^{2+} complex may convert to **Cou-COOH** (Fig.S3).

Further fluorescence titration of **Cou-P** by Cu^{2+} shows similar phenomena. Titration of **Cou-P** by Cu^{2+} exhibits a linear emission decrease with $c_{\text{Cu}^{2+}}$, and the fluorescence of **Cou-P** was quenched efficiently when the $c_{\text{Cu}^{2+}}/c_{\text{Cou-P}}$ ratio attained 1 (Fig.3a). However, after the $c_{\text{Cu}^{2+}}/c_{\text{Cou-P}}$ ratio attained 1, upon addition of another 0.1 eq. Cu^{2+} to the solution of **Cou-P**/ Cu^{2+} complex, a new excitation band centered at 403 nm appeared and the intensity enhanced gradually in a time-dependent manner (Fig.3b). After 300 minutes, the fluorescence intensity at 403 nm (I_{403}) was reached its maximum. Further addition of EDTA could not eliminate the fluorescence (Fig.S4). This result demonstrates that **Cou-P**/ Cu^{2+} complex might have undergone Cu^{2+} -catalyzed chemical reactions.

To further verify the recognition mechanism of probe **Cou-P** for Cu^{2+} , the reaction product of **Cou-P** with Cu^{2+} was characterized by the ESI-MS spectrometry. After addition of 1.1 eq $\text{Cu}(\text{NO}_3)_2$ for 60 min, ESI-MS of **Cou-P** shows a peak assigned to $[\text{Cou-P-H}^+ + \text{Cu}^{2+} + \text{CH}_3\text{OH}]^+$ (Fig.S5). After 300 min, there are three prominent peaks, 341.5 assigned to $[\text{3-H}^+ + \text{Cu}^{2+} + \text{H}_2\text{O}]^+$, 171.42 assigned to $[(\text{3} + \text{Cu}^{2+} + \text{H}_2\text{O})/2]^+$, 251.33

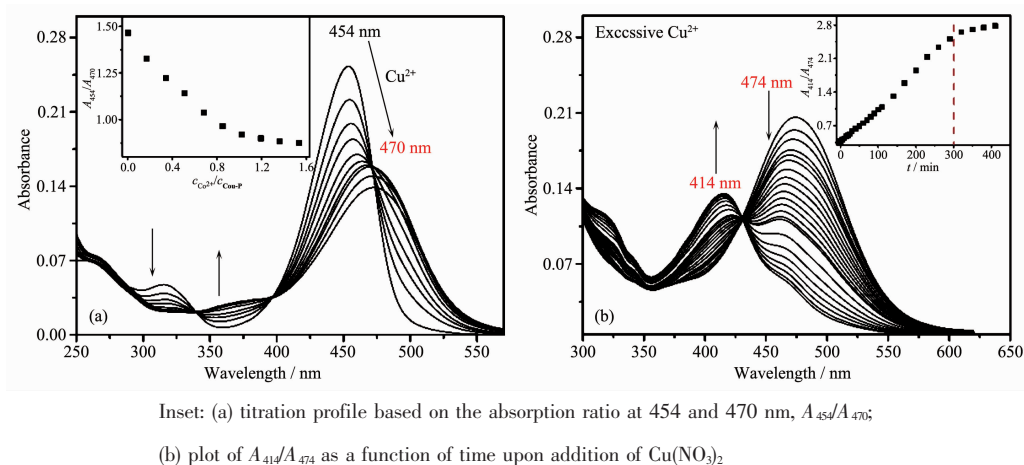
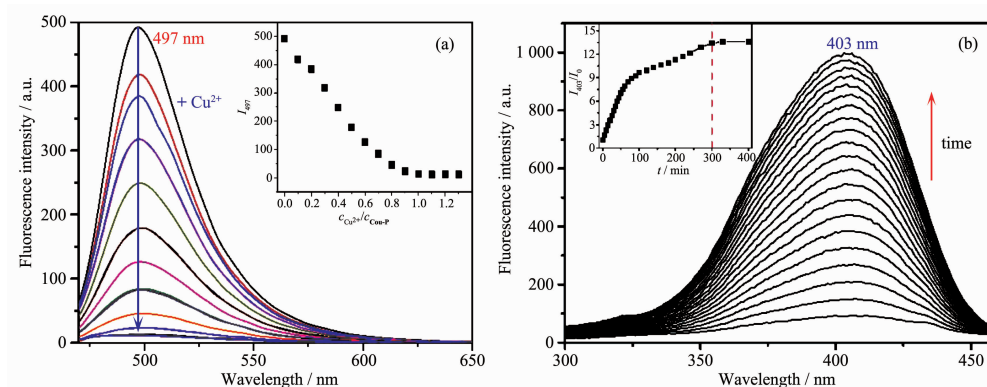


Fig.2 (a) Absorbance spectra of $10\text{ }\mu\text{mol}\cdot\text{L}^{-1}$ **Cou-P** in HEPES buffer obtained by adding 0~1.6 eq. $\text{Cu}(\text{NO}_3)_2$ ($1.2\text{ mmol}\cdot\text{L}^{-1}$) solution; (b) Time-dependent UV-Vis absorption spectra of $20\text{ }\mu\text{mol}\cdot\text{L}^{-1}$ **Cou-P** in HEPES buffer obtained by adding excessive $\text{Cu}(\text{NO}_3)_2$ ($100\text{ }\mu\text{mol}\cdot\text{L}^{-1}$) solution

assigned to $[4+\text{MeOH}+\text{Na}^+]^+$, respectively (Fig.4). The isotopic distribution of peak at 341.5 matches with the results of ISOPRO 3.0 simulation, which further indicates the reaction product of **Cou-P** with Cu^{2+} . This result is consistent with the experimental results of spectroscopy.

Thus, the coordination of Cu^{2+} to picolinic ester in probe **Cou-P** is essential for the Cu^{2+} -promoted hydrolytic cleavage of **Cou-P** to **Cou-COOH** (**3**). Based on the above results, a detailed recognition mechanism of probe **Cou-P** for Cu^{2+} was proposed as shown in Scheme 2.



Inset: (a) titration profile based on the emission intensity at 497 nm, I_{497} , $\lambda_{em}=460$ nm; (b) time-dependent fluorescence at 403 nm, $\lambda_{em}=510$ nm, slit width= $d_{ex}=d_{em}=4.0$ nm, PMT voltage=950 V

Fig.3 (a) Emission spectra of $10 \mu\text{mol}\cdot\text{L}^{-1}$ **Cou-P** in HEPES buffer obtained by adding aliquots of $2.5 \mu\text{L}$ $\text{Cu}(\text{NO}_3)_2$ ($1.2 \text{ mmol}\cdot\text{L}^{-1}$) solution; (b) Time-dependent fluorescent excitation spectra of $10 \mu\text{mol}\cdot\text{L}^{-1}$ **Cou-P** in HEPES buffer after addition of 1.1 eq. $\text{Cu}(\text{NO}_3)_2$

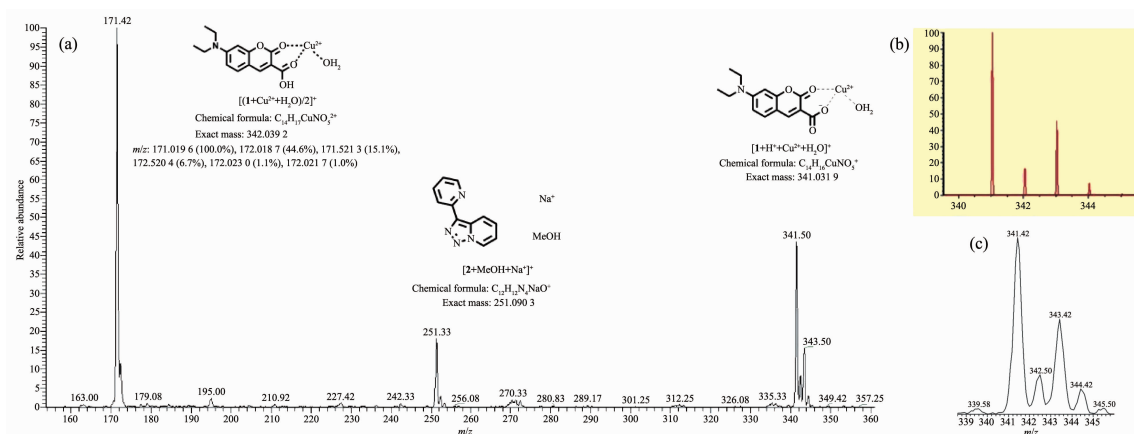
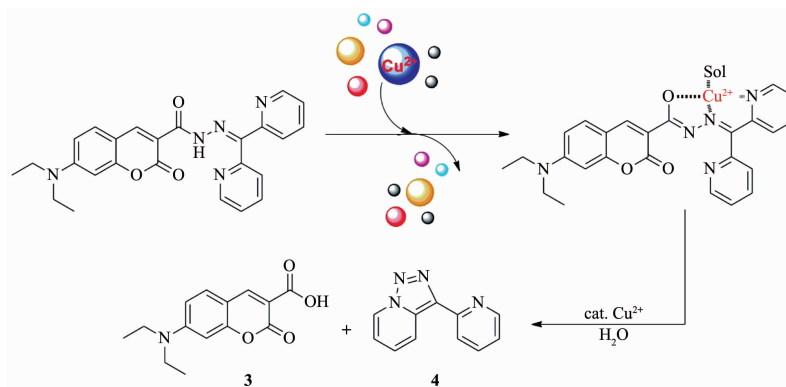


Fig.4 (a) ESI-MS of **Cou-P** in $\text{MeOH}/\text{H}_2\text{O}$ (1:1, V/V) after addition of 1.1 eq. $\text{Cu}(\text{NO}_3)_2$ for 5 h; (b) Corresponding simulated one for $[3-\text{H}^++\text{Cu}^{2+}+\text{H}_2\text{O}]^+$; (c) Determined isotopic distribution patterns of the peak with m/z of 341.50

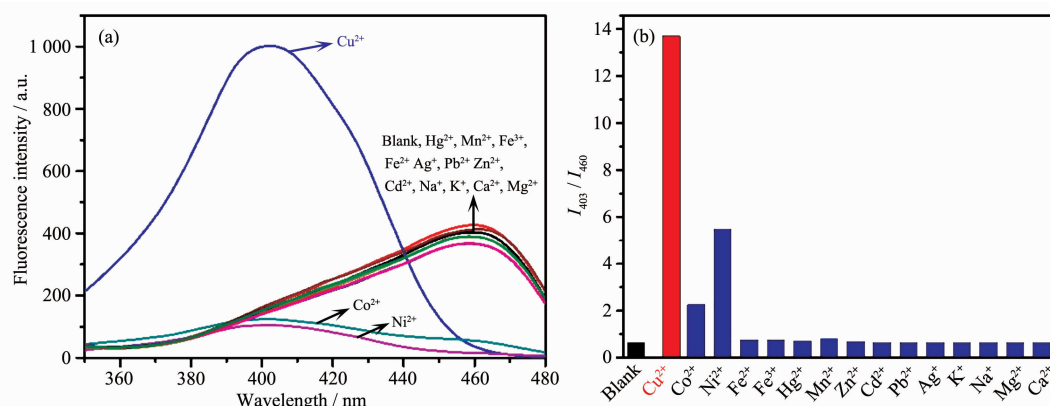


Scheme 2 Proposed mechanism of Cu^{2+} -catalysed reaction of **Cou-P**

2.3 Cu²⁺ detection selectivity

Selectivity is a crucial parameter to assess the performance of the developed probes. Therefore, the selectivity experiments of **Cou-P** were extended to a variety of biological-related species including common cations (K⁺, Na⁺, Mg²⁺, Ca²⁺, Co²⁺, Ni²⁺, Fe²⁺, Fe³⁺, Hg²⁺, Mn²⁺, Zn²⁺, Cd²⁺, Pb²⁺ and Ag⁺). As shown in Fig.5a, only introduction of Cu²⁺ could cause apparent fluorescence intensity changes of the probe **Cou-P** solution, most of the tested cation did not induce any emission

enhancement at 403 nm. According to the value of I_{403}/I_{460} , Cu²⁺ can induce 13-fold fluorescence enhancement, and Co²⁺ and Ni²⁺ also induce very minor enhancement due to fluorescence quenching at 460 nm (Fig.5b). Moreover, the abundant metal cations in natural water such as Na⁺, K⁺, Ca²⁺ and Mg²⁺ do not result in distinct emission either. This provides probe **Cou-P** the advantage in sense Cu²⁺ in samples containing abundant Na⁺, K⁺, Ca²⁺, and Mg²⁺, such as living cells.



Final concentration for Cd²⁺, Zn²⁺, Co²⁺, Cu²⁺, Fe²⁺, Fe³⁺, Hg²⁺, Mn²⁺, Ni²⁺ and Pd²⁺ is 20 $\mu\text{mol}\cdot\text{L}^{-1}$, for Na⁺, K⁺, Ca²⁺ and Mg²⁺ is 10 $\text{mmol}\cdot\text{L}^{-1}$

Fig.5 (a) Excitation spectra of **Cou-P** ($10\ \mu\text{mol}\cdot\text{L}^{-1}$) in the presence of various metal ions in HEPES buffer ($50\ \text{mmol}\cdot\text{L}^{-1}$, $0.1\ \text{mol}\cdot\text{L}^{-1}\ \text{KNO}_3$, pH 7.2); (b) Ratio of fluorescence intensity at 403 and 460 nm of $10\ \mu\text{mol}\cdot\text{L}^{-1}$ **Cou-P** induced by different metal ions in HEPES buffer

2.4 Cell cytotoxicity and confocal fluorescence imaging

The cytotoxicity of probe **Cou-P** in MCF-7 cells was evaluated by MTT assays with the concentration of the probe ranging from 2 to $50\ \mu\text{mol}\cdot\text{L}^{-1}$ (Fig.S6). The results show that **Cou-P** is of low cytotoxicity to cultured cells and should be safe when used for bioimaging of Cu²⁺.

Based on the favorable features of **Cou-P** including visible emission, high selectivity for Cu²⁺ and low toxicity, the potential utility of **Cou-P** to visualize Cu²⁺ in living cells was investigated. As shown in Fig.6, MCF-7 cells incubated with **Cou-P** ($10\ \mu\text{mol}\cdot\text{L}^{-1}$) alone for 30 min at 37 °C exhibited no observable fluorescence. However, when cells were further incubated with Cu²⁺ ($200\ \mu\text{mol}\cdot\text{L}^{-1}$) for 300 min

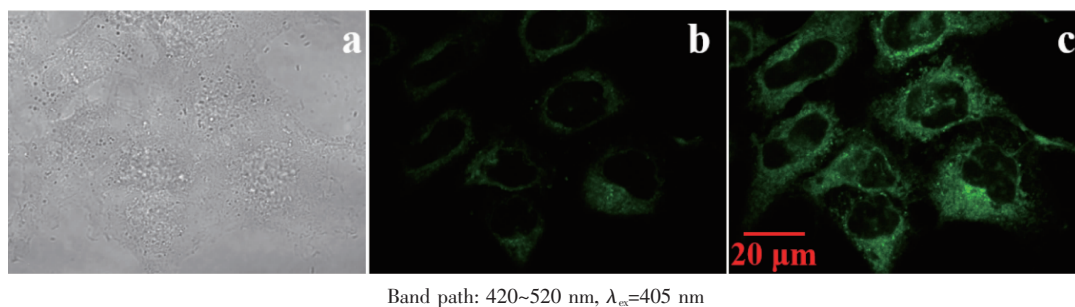


Fig.6 Confocal fluorescence images of intracellular Cu²⁺ in MCF-7 cells with **Cou-P**-staining: (a) Bright-field transmission images; (b) MCF-7 cells incubated with **Cou-P** ($10\ \mu\text{mol}\cdot\text{L}^{-1}$) at 37 °C for 30 min; (c) Stained cells further exposed to $200\ \mu\text{mol}\cdot\text{L}^{-1}\ \text{Cu}(\text{NO}_3)_2$ solution at 37 °C for 300 min

at 37 °C, remarkable intracellular fluorescence could be observed. These results indicate that probe **Cou-P** is permeable to cell membrane and suitable for imaging Cu²⁺ in living cells.

3 Conclusions

In summary, we successfully developed a new reaction fluorescent probe for detecting Cu²⁺. Probe **Cou-P** exhibits a fluorescence “turn-on” recognition process for Cu²⁺. The recognition mechanism of probe **Cou-P** for Cu²⁺ was investigated by UV-Vis, fluorescence and ESI-MS spectrometry. In application, **Cou-P** shows low cytotoxicity and good membrane permeability. More importantly, **Cou-P** was successfully used for the detection of Cu²⁺ in living cells, indicating its great potential for Cu²⁺ detection in biological science.

Supporting information is available at <http://www.wjhxsb.cn>

References:

- [1] Martínez-Máez R, Sancenón F. *Chem. Rev.*, **2003**,**103**:4419-4476
- [2] Thomas S W, Joly G D, Swager T M. *Chem. Rev.*, **2007**,**107**: 1339-1386
- [3] Kim S K, Lee D H, Hong J I, et al. *Acc. Chem. Res.*, **2009**, **42**:23-31
- [4] Xu Z C, Chen X Q, Kim H N, et al. *Chem. Soc. Rev.*, **2010**, **39**:127-137
- [5] Zhou Y, Xu Z C, Yoon J. *Chem. Soc. Rev.*, **2011**,**40**:2222-2235
- [6] Vendrell M, Zhai D T, Er J C, et al. *Chem. Rev.*, **2012**,**112**: 4391-4420
- [7] Liu Z P, He W J, Guo Z J. *Chem. Soc. Rev.*, **2013**,**42**:1568-1600
- [8] Prohaska J R, Gybina A A. *J. Nutr.*, **2004**,**134**:1003-1006
- [9] Davis A V, O'Halloran T V. *Nat. Chem. Biol.*, **2008**,**4**:148-151
- [10] Que E L, Domaille D W, Chang C J. *Chem. Rev.*, **2008**,**108**: 1517-1549
- [11] Thiele D J, Gitlin J D. *Nat. Chem. Biol.*, **2008**,**4**:145-147
- [12] Robinson N J, Winge D R. *Annu. Rev. Biochem.*, **2010**,**79**: 537-562
- [13] Cuajungco M P, Lees G J. *Neurobiol. Dis.*, **1997**,**4**:137-169
- [14] Bush A I. *Curr. Opin. Chem. Biol.*, **2000**,**4**:184-191
- [15] Valentine J S, Hart P J. *Proc. Natl. Acad. Sci. USA*, **2003**, **100**:3617-3622
- [16] Brown D R, Kozłowski H. *Dalton Trans.*, **2004**,**13**:1907-1917
- [17] Millhauser G L. *Acc. Chem. Res.*, **2004**,**37**:79-85
- [18] Frederickson C J, Koh J Y, Bush A I. *Nat. Rev. Neurosci.*, **2005**,**6**:449-462
- [19] Gaggelli E, Kozłowski H, Valensin D, et al. *Chem. Rev.*, **2006**,**106**:1995-2044
- [20] Lutsenko S, Gupta A, Burkhead J L, et al. *Arch. Biochem. Biophys.*, **2008**,**476**:22-32
- [21] Kaler S G. *Nat. Rev. Neurol.*, **2011**,**7**:15-29
- [22] Domaille D W, Que E L, Chang C J. *Nat. Chem. Biol.*, **2008**,**4**:168-175
- [23] World Health Organization. *Guidelines for Drinking-Water Quality. 4th Ed.* Geneva: World Health Organization, **2017**: 341
- [24] Wang X B, Ma X Y, Yang Z, et al. *Chem. Commun.*, **2013**, **49**:11263-11265
- [25] Kang D E, Lim C S, Kim J Y, et al. *Anal. Chem.*, **2014**,**86**: 5353-5359
- [26] Sharma N, Reja S I, Bhalla V, et al. *Dalton Trans.*, **2014**,**43**: 15929-15936
- [27] Han Y Y, Ding C Q, Zhou J, et al. *Anal. Chem.*, **2015**,**87**: 5333-5339
- [28] Kaur M, Ahn Y H, Choi K, et al. *Org. Biomol. Chem.*, **2015**, **13**:7149-7153
- [29] Li S, Zhang D, Xie X Y, et al. *Sens. Actuators B*, **2016**,**224**: 661-667
- [30] Jiang H, Li Z J, Kang Y F, et al. *Sens. Actuators B*, **2017**, **242**:112-117
- [31] Li Y Y, Sun M T, Zhang K, et al. *Sens. Actuators B*, **2017**, **243**:36-42
- [32] Liu L L, Dan F J, Liu W J, et al. *Sens. Actuators B*, **2017**, **247**:445-450
- [33] Yoon J W, Chang M J, Hong S, et al. *Tetrahedron Lett.*, **2017**,**58**:3887-3893
- [34] FAN Fang-Lu(范方禄), JING Jin-Qiu(靖金球), CHEN Xue-Mei(陈雪梅). *Chinese J. Inorg. Chem.* (无机化学学报), **2015**,**31**(3):548-554
- [35] Lin W Y, Yuan L, Tan W, et al. *Chem. Eur. J.*, **2009**,**15**: 1030-1035
- [36] Li N, Xiang Y, Tong A. *Chem. Commun.*, **2010**,**46**:3363-3365
- [37] Cheng J H, Zhang Y H, Ma X F, et al. *Chem. Commun.*, **2013**,**49**:11791-11793
- [38] Huang L Y, Gu B, Su W, et al. *RSC Adv.*, **2015**,**5**:76296-76301

- [39]Hu X X, Zheng X L, Fan X X, et al. *Sens. Actuators B*, **2016**,**227**:191-197
- [40]Li D X, Sun X, Huang J M, et al. *Dyes Pigm.*, **2016**,**125**: 185-191
- [41]Sun J, Wang B, Zhao X, et al. *Anal. Chem.*, **2016**,**88**:1355-1361
- [42]Tan W B, Leng T H, Lai G Q, et al. *J. Photochem. Photobiol. A*, **2016**,**324**:81-86
- [43]Tang J, Ma S G, Zhang D, et al. *Sens. Actuators B*, **2016**, **236**:109-115
- [44]Wang B G, Cui X Y, Zhang Z Q, et al. *Org. Biomol. Chem.*, **2016**,**14**:6720-6728
- [45]Zhu D J, Luo Y H, Shuai L, et al. *Tetrahedron Lett.*, **2016**, **57**:5326-5329
- [46]Zheng X L, Ji R X, Cao X Q, et al. *Anal. Chim. Acta*, **2017**, **978**:48-54
- [47]Gu B, Huang L Y, Xu Z F, et al. *Sens. Actuators B*, **2018**, **273**:118-125
- [48]Sirilaksanapong S, Sukwattanasinitt M, Rashatasakhon P. *Chem. Commun.*, **2012**,**48**:293-295
- [49]Zhao C C, Feng P, Cao J, et al. *Org. Biomol. Chem.*, **2012**, **10**:3104-3109
- [50]Yang C Y, Chen Y, Wu K, et al. *Anal. Methods*, **2015**,**7**: 3327-3330
- [51]Tang L J, He P, Zhong K L, et al. *Spectrochim. Acta Part A*, **2016**,**169**:246-251
- [52]Zhu D J, Luo Y H, Yan X W, et al. *RSC Adv.*, **2016**,**6**: 87110-87114
- [53]Zhang H T, Feng L, Jiang Y, et al. *Biosens. Bioelectron.*, **2017**,**94**:24-29